HHS Public Access

Author manuscript

Am J Drug Alcohol Abuse. Author manuscript; available in PMC 2023 June 30.

Published in final edited form as:

Am J Drug Alcohol Abuse. 2021 September 03; 47(5): 581–589. doi:10.1080/00952990.2021.1954189.

Differential expression and transcription factor binding associated with genotype at a pharmacogenetic variant in *OPRD1*

Richard C. Crist, PhD[1], **Gabriella Arauco-Shapiro, MS**[1], **Alexander Zhang, BS**[1], **Benjamin C. Reiner, PhD**[1], **Wade H. Berrettini, MD, PhD**[1,2], **Glenn A. Doyle, PhD**[1]

[1]Department of Psychiatry, University of Pennsylvania Perelman School of Medicine, Philadelphia, PA

[2]Geisinger Clinic, Danville, PA

Abstract

Background: The functional mechanism is unknown for many genetic variants associated with substance use disorder phenotypes. Rs678849, an intronic variant in the delta-opioid receptor gene (*OPRD1*), has been found to predict regional brain volume, addiction risk, and the efficacy of buprenorphine/naloxone in treating opioid use disorder. The variant has also been implicated as an expression quantitative trait locus (eQTL) for several genes.

Objectives: The objective of this study was to identify functional differences between the two alleles of rs678849 *in vitro*. We hypothesize that the two alleles of rs678849 have different effects on transcriptional activity due to differential interactions with transcription factors.

Methods: 15bp regions containing the C or T alleles of rs678849 were cloned into luciferase constructs and transfected into BE(2)C neuroblastoma cells to test the effect on transcription. Electrophoretic mobility shift assays (EMSA) using nuclear lysates from BE(2)C cell or human postmortem medial prefrontal cortex were used to identify proteins that differentially bound the two alleles.

Results: At 24 hours post-transfection, the C allele construct had significantly lower luciferase expression than the T allele construct and empty vector control (ANOVA $p < 0.001$). Proteomic analysis and supershift assays identified XRCC6 as a transcription factor specifically binding the C allele, whereas hnRNP D0 was found to specifically bind the T allele.

Conclusion: These functional differences between the C and T alleles may help explain the psychiatric and neurological phenotype differences predicted by rs678849 genotype and the potential role of the variant as an eQTL.

Corresponding Author Richard C. Crist, Ph.D., University of Pennsylvania School of Medicine, Department of Psychiatry, Center for Neurobiology and Behavior, Translational Research Laboratories, 125 South 31st Street, Room 2207, Philadelphia, PA 19104, Office: (215) 746-3665, Fax: (215) 573-2041, crist@pennmedicine.upenn.edu.

Disclosure of Interest

The authors report no conflict of interest.

INTRODUCTION

Candidate gene studies and genome-wide association studies (GWAS) have identified a growing number of genetic polymorphisms associated with addiction phenotypes. Limited functional data are available for most of these variants. For example, genetic studies of alcoholism and alcohol consumption reproducibly identify a significant locus in the *ADH1B* gene, which encodes an alcohol dehydrogenase enzyme (1-3). The minor allele of the presumptive causative variant identified in these studies is associated with increased alcohol metabolism. Minor allele carriers consume less alcohol on average and are less likely to develop an alcohol use disorder (1-3). This type of mechanistic data provides validity to the original genetic associations and may produce additional biomarkers or therapeutic targets. Only a small number of similar examples exist in the fields of opioid use disorder (OUD) risk and treatment. A 3' UTR variant in the mu-opioid receptor gene (*OPRM1*) was found to predict methadone efficacy in treating OUD (4). A miRNA was subsequently shown to bind only one of the two alleles *in vitro*, resulting in translational repression. Hancock *et al.* identified functional addiction-related polymorphisms with a different approach, first using the BrainCloud dataset to identify expression quantitative trait loci (eQTLs) for cortical expression of *OPRM1* and then performing case-control analyses with those variants (5). This method allowed them to identify a functional intronic variant, rs3778150, associated with OUD and replicate that association. In a Han Chinese population, the severity of heroin dependence was associated with rs9479757, another intronic *OPRM1* variant that is in perfect linkage disequilibrium with rs3778150 ($r^2 = 1.0$, D' = 1.0) in that ethnic group (6). Genotype at rs9479757 was found to alter alternative splicing through a mechanism mediated by hnRNPH (6). Despite these examples, most addiction-related variants currently have no clear mechanistic information, representing a significant knowledge gap that needs to be addressed.

We previously observed an association between the *OPRD1* intronic variant rs678849 and the percentage of opioid positive urine drug screens in African-Americans being treated for OUD with buprenorphine/naloxone agonist replacement therapy (7). This pharmacogenetic effect was replicated in an independent cohort (8). More recently, rs678849 genotype was found to predict the effectiveness of extended-release buprenorphine in preventing opioid use in European-Americans, but not African-Americans, with OUD (9). Genotype at rs678849 has also been associated with cocaine dependence in African-Americans and OUD in Iranians (10, 11). An additional analysis found the variant to predict regional brain volume in individuals of European descent (12). That study also found healthy elderly people with the C/C genotype to have a significantly lower tau/beta-amyloid ratio than individuals with the C/T or T/T genotypes (12).

Little is known about the mechanisms by which rs678849 affects these various human phenotypes. Understanding the functional consequences of rs678849 genotype could provide insight into the biology of addiction and other phenotypes, and help identify additional markers of treatment efficacy. Here we report the ability of loci containing the C or T alleles of rs678849 to act as transcriptional modulators *in vitro* and the identity of proteins binding to the different alleles.

MATERIALS AND METHODS

Cell Culture

BE(2)C neuroblastoma cells were purchased from ATCC (catalog #: CRL-2268). STR analysis was used to verify the identity of the cell line. The lot used for these experiments tested negative for mycoplasma contamination. Cells were cultured in 24-well plates in a 1:1 mixture of Eagle's Minimum Essential Medium and Ham's F-12 Medium with 10% fetal bovine serum.

Luciferase Assays

The 15bp regions containing the C or T allele of rs678849 (TCAAAAG[C/T]ACCTGCT) were cloned into the *Bam*HI site downstream of the *luc2* gene in the pGL4.23 vector (Promega) (Figure 1A). Successful integration of the appropriate region in each construct was confirmed by Sanger sequencing. Transit LT1 reagent (Mirus Bio) was used to transfect BE(2)C cells at 60-80% confluence with the firefly luciferase constructs containing the C or T allele locus and *Renilla* luciferase vector pGL4.74 (Promega) to control for transfection efficiency between replicates. Empty pGL4.23 vector transfections were used as a control. Mock transfections without plasmid were performed to control for any background luminescence. Transfections were performed in triplicate in each of three independent experiments (n = 8-9 for all conditions). Luciferase activities were assessed on a GloMax 20/20 at 24 hours post-transfection using a dual-luciferase report assay system (Promega) as previously described (4). Results for the rs678849-C and rs678849-T constructs were normalized to the empty vector control. Data were analyzed by one-way ANOVA and post-hoc Tukey HSD tests using JMP v12.0.

Electrophoretic Mobility Shift Assays (EMSA)

Double-stranded DNA probes (15bp) for both alleles of rs678849 were synthesized, annealed, and purified by Integrated DNA Technologies (C allele sense sequence: 5'-TCAAAAGCACCTGCT-3'; T allele sense sequence: 5'-TCAAAAGTACCTGCT-3'). The fluorophore Cy3 was conjugated to the 3' end of the sense strands for each probe. Unlabeled versions of the C and T allele probes were also produced, as well as an unlabeled competitor probe containing the murine Oct1 consensus sequence (TCGAATGCAAATCAC). BE(2)C nuclear lysate was obtained using a Nuclear Extraction Kit (AbCam). Postmortem medial prefrontal cortex tissue was received from NIH NeuroBioBank at the University of Maryland. Tissue was homogenized in a Dounce homogenizer and nuclear lysate was again obtained using the Nuclear Extraction Kit. Double-stranded T probe (2 pmol) was incubated with 20μg nuclear lysate for 25 min at room temperature in 20μL modified 1X Cold Spring Harbor EMSA binding buffer (30mM NaCl, 5mM HEPES-KOH (pH 7.6), 1.2mM DTT, 20μM EDTA, 83.3nM poly-dIdC). Double-stranded C probe incubation was performed as above but using dephosphorylated lysate to remove a prominent non-specific band (Figure 2A). Dephosphorylated lysate was generated by incubating BE(2)C or medial prefrontal cortex nuclear lysate with 1U calf intestinal alkaline phosphatase per 80ug lysate (NEB) for 30 minutes at 37°.

To test the specificity of binding proteins, EMSA reactions were also performed in the presence of 300pmol of unlabeled C probe, unlabeled T probe, or Oct1 duplex as competitors. Glycerol (1μl) was added to each reaction following incubation and the reactions were separated by electrophoresis at 15mA at 4°C on 8% polyacrylamide gels. Gels were imaged on a Typhoon TRIO scanner (Amersham Biosciences). EMSA bands of specific complexes were excised and proteins of interest were identified at the University of Pennsylvania Quantitative Proteomics Resource Core using LC-MS/MS. To confirm the identity of the protein binding to the T allele, MYC-DDK-tagged recombinant hnRNP D0 (isoform 3) was used in place of nuclear lysate (Origene; #RC200660). All EMSA reactions were performed in triplicate. Regions of interest were quantified using ImageJ v1.53e with normalization to lane background. Quantification data were analyzed by one-way ANOVA and post-hoc Tukey HSD tests in VassarStats.

Experiments involving human tissue were approved by the NeuroBioBank Brain and Tissue Repositories and were carried out in accordance with all relevant regulations. Informed consent was obtained from all tissue donors or their next-of-kin under protocols reviewed and approved by the University of Maryland institutional review board.

Supershift Assays

Following incubation of the EMSA reactions with 300pmol of Oct1 duplex, 1ul of antibody was added to the reaction and incubated for an additional 25min at room temperature. Reactions were separated and analyzed as described above. The following antibodies were used: α-pan-hnRNP (detects hnRNP D0, hnRNP D-like, and hnRNP A/B; Santa Cruz Biotechnology, #sc-166577), α-hnRNP A1 (Abcam, #ab5832), α-TCF3 (Abcam, # ab229605), α-XRCC6 (Cell Signaling Technology, # 4104), and α-XRCC6/XRCC5 (Invitrogen, #MA1-21818). Supershift reactions with BE(2)C lysate were performed in triplicate. Regions of interest were quantified and statistically analyzed as described above for EMSA. Due to the confirmatory nature of the prefrontal cortex experiment and limited amounts of tissue lysate, supershift assays with prefrontal cortex were performed once on a single sample and the presence or absence of the relevant bands was assessed qualitatively.

RESULTS

The C allele of rs678849 acts as a silencer element in an in vitro luciferase system

The 15bp genomic regions containing the C or T allele of rs678849 were cloned downstream of the firefly luciferase gene in the pGL4.23 vector (Figure 1A). To test the effects of the two alleles on transcription, BE(2)C neuroblastoma cells were transfected with the C allele construct, T allele construct, or the empty vector control. At 24 hours post-transfection, cells transfected with the C allele construct had significantly less luciferase expression than cells transfected with either the T allele construct or the empty vector control (ANOVA $p < 0.001$; $n = 8$-9 for all conditions) (Figure 1B). No difference in luciferase expression was observed between cells transfected with the T allele and empty vector (Figure 1B).

The rs678849 C and T allele probes are bound by different protein complexes in BE(2)C nuclear lysate

Since the rs678849 loci were downstream of the luciferase gene in the constructs, the observed expression differences are most likely the result of differential binding of transcription factors to the two alleles. To identify the relevant factors, BE(2)C nuclear lysate was incubated with Cy3-labeled probes representing the 15bp C and T allele regions used in the luciferase assays. Electrophoretic mobility shift assays (EMSA) demonstrated that both of the probes formed DNA:protein complexes (Figure 2A-B). Competition with unlabeled C probe, T probe, or a 15bp sequence containing a murine Oct1 site was used to determine the specificity of protein binding. The T allele formed a series of sequence-specific complexes (T1) that were outcompeted by unlabeled T probe but not unlabeled C probe (n=3, ANOVA $p < 0.01$) (Figure 2A). Other non-specific DNA:protein complexes were also formed.

For the C allele EMSA, the nuclear lysate was dephosphorylated, allowing us to eliminate a prominent non-specific DNA:protein complex (Figure 2A-B). The C allele probe was bound by a sequence-specific complex (C1) that was previously difficult to observe due to its migration at approximately the same location as the prominent non-specific DNA:protein complex (n=3, ANOVA $p < 0.01$) (Figure 2B). No equivalent complex was observed when the T probe was incubated with dephosphorylated lysate (data not shown). Additional non-specific complexes were also observed in the C allele reactions.

The T allele-specific complex, T1, contains hnRNP D0

LC/MS-MS analysis indicated that the most abundant protein in the T1 complex was isoform 3 of hnRNP D0 (Supplemental Table 1). Incubation of the T allele EMSA reaction with an α-pan-hnRNP antibody designed using an hnRNP D0 epitope eliminated the top two bands of the T1 series, whereas no effect was observed in the presence of α-hnRNP A1 or α-TCF3 antibodies (Figure 3A). These results suggest that these complexes both contain hnRNP D0. Since the α-pan-hnRNP antibody is known to also detect the related proteins hnRNP D-like and hnRNP A/B, additional EMSA reactions were performed with recombinant hnRNP D0 (isoform 3) in place of nuclear lysate. As shown in Figure 3C, the recombinant protein bound the T allele probe. Some minor binding to the C allele was also present (Figure 3B); however, the relative strength of the EMSA bands supports the hypothesis that hnRNP D0 has a significantly higher affinity for the T allele than the C allele.

The C allele-specific complex, C1, contains XRCC6 (Ku70)

Proteomic analysis identified XRCC6 (aka Ku70) as part of the C1 complex (Supplemental Table 2). Formation of the C1 complex was disrupted by addition of α-XRCC6 antibody to the EMSA reaction, but not by addition of α-TCF3 or α-pan-hnRNP antibodies (Figure 3D). These results indicate that C1 contains XRCC6. XRCC6 frequently binds DNA as a heterodimer with XRCC5 (aka Ku80); however, incubation of the C allele EMSA reaction with an antibody specific to the XRCC6/XRCC5 heterodimer did not affect C1 complex formation (Figure 3D). Unlike the α-pan-hnRNP antibody, the manufacturer did not predict the α-XRCC6 antibody to have off-target binding. Prior use of the antibody in the literature

also showed no evidence of off-target interactions (13, 14). Confirmatory EMSA using recombinant XRCC6 was therefore not performed.

XRCC6 and hnRNP D0 interact with the rs678849 locus in nuclear lysate from human postmortem brain

To test the applicability of our findings to human tissue, EMSA reactions were also performed using nuclear lysate from African-American postmortem medial prefrontal cortex (mPFC), a brain region whose function is disrupted in individuals with substance use disorders (15). Allele-specific bands at approximately the same sizes as C1 and T1 were present in the mPFC reactions (Figure 4A-B). Although the second slowest migrating band in T1 was the most prominent in the BE(2)C assays, the slowest band was the most prominent when using mPFC lysate (data not shown). This difference is likely due to the relative abundance of different post-translational modifications or splice variants. Qualitative assessment of supershift assays with α-XRCC6 and α-pan-hnRNP antibodies confirmed that XRCC6 and D0 were present in C1 and T1, respectively, in human brain tissue (Figure 4A-B).

DISCUSSION

Our results indicate that the C and T alleles of rs678849, a variant repeatedly associated with buprenorphine treatment outcomes (7-9) and other addiction phenotypes (10, 11), have differential effects on expression and bind distinct protein complexes. Proteomic analyses identified hnRNP D0 as part of the T1 complex. The protein was originally described as an RNA binding protein, but more recent work has shown hnRNP D0 to have the ability to bind dsDNA and function as a transcription factor (16-20). A consensus DNA binding sequence for hnRNP D0 has not been determined, but known binding sites in *CR2* and *BDNF* have noticeable similarities to the rs678849 locus (Figure 5). In the case of *BDNF*, hnRNP D0 was shown to preferentially bind the T allele of rs12291063 compared to the C allele (17). This polymorphism's position in the binding site is similar to that of rs678849 (Figure 5). The findings in *CR2*, *BDNF*, and other genes demonstrate dsDNA binding specifically for isoform 3 of hnRNP D0 (aka hnRNP D0B) (17, 18, 20). This splice variant is localized to the nucleus instead of the cytoplasm due a lack of exon 7, which encodes a nuclear export sequence. Our proteomic analysis is consistent with these results since we specifically identified this isoform as a component of T1 and recombinant isoform 3 hnRNP D0 protein bound preferentially to the T allele of rs678849 via EMSA (Figure 3B).

Although hnRNP D0 has been shown to act as a transcription factor, our luciferase experiments found no difference in expression between the T allele of rs678849 and the empty vector control (Figure 1B). The rs678849 locus *in vivo* exists in the context of other cis regulatory elements that are adjacent to the locus. Regulatory elements also often physically interact with other elements or promoter regions through the three-dimensional conformation of the chromosome. Other loci (*e.g.* the *OPRD1* promoter) were not present in the *in vitro* experiments and, therefore, direct and indirect interactions with rs678849 that were potentially relevant to transcriptional regulation by hnRNP D0 may not have been well-modeled.

Our analyses also identified XRCC6 as a component of the C1 complex (Figure 3D). XRCC6 is most known as a binding partner for XRCC5 and the two proteins function as part of the non-homologous end-joining machinery (21, 22). However, XRCC6/XRCC5 heterodimers have also been shown to regulate transcription through binding to promoter regions. The protein complex acts as a repressor of transcription of the GBP and IL-2 genes in human erythrocytes and T-cells, respectively (23, 24). Upregulation of other genes has also been associated with XRCC6/XRCC5 binding, notably in the presence of other binding partners such as AP-2 family members (25). Transcriptional regulation by XRCC6/XRCC5 has been observed in murine cells, suggesting a conserved role for XRCC6 as a transcription factor and providing evidence for the existence of additional binding partners (26, 27). As with hnRNP D0, the consensus DNA binding site for the XRCC6/XRCC5 dimer is not fully determined but the protein complex appears to have significant flexibility based on known binding sites (23).

The known transcriptional regulation by XRCC6 involves the XRCC6/XRCC5 heterodimer; however, we were not able to confirm the presence of XRCC5 in the C1 complex. While there is currently no evidence that XRCC6 regulates transcription as a monomer, the protein is known to have functions independent of XRCC5. Mice lacking Xrcc5 or Xrcc6 do not have identical phenotypic profiles: *Xrcc5* knockout animals demonstrate accelerated aging, whereas *Xrcc6* knockouts develop thymic lymphoma (28, 29). XRCC6 is also known to have other binding partners, including Cyclin E and Bax (30, 31). Binding of XRCC6 to the C allele of rs678849 may therefore require unidentified proteins besides XRCC5. Furthermore, although the XRCC6/XRCC5 antibody did not disrupt formation of C1 (Figure 3D), we cannot completely exclude the possibility that XRCC5 is contained in the complex. For example, additional proteins included in C1 may have blocked the epitope targeted by the antibody or the phosphatase treatment may have disrupted binding of this specific antibody. Additional proteomic analyses are still required to determine the remaining components of the C1 complex.

Our luciferase assay results suggest that rs678849-C is acting as a silencer element (Figure 1B), but it remains unclear what gene or genes might be affected. Data from the BrainSeq consortium indicates that rs678849 is an expression quantitative trait locus (eQTL) for the *PHACTR4* gene in dorsolateral prefrontal cortex (32). Additional analyses from the Genotype-Tissue Expression (GTEx) project identified rs678849 as an eQTL for several genes in different tissues, including *PHACTR4*, *ATPIF1*, and *RP5-1092A3.4* (33). The C allele of rs678849 is associated with lower expression in all of these associations from BrainSeq and GTEx, aligning with our data and making all three genes viable candidates for an rs678849 effect. While *RP5-1092A3.4* was the only gene in GTEx to have a significant eQTL effect in brain tissue, this may be the result of the much larger sample sizes for certain tissues in that database compared to the various brain regions. *OPRD1* itself also remains a potential candidate. Although expression of *OPRD1* was not associated with rs678849 genotype in GTEx, the lack of observed effect may be due to the low levels of *OPRD1* transcript in bulk brain tissue lysates, diminishing statistical power to detect an association.

Identifying both the relevant transcription factors and the target gene(s) regulated by rs678849-C could aid in identifying the time and place in which rs678849 genotype is

relevant. It is currently unclear whether the rs678849 effects occur in adulthood or in the developing brain, but some of the candidate genes have specific expression patterns that could provide evidence for one or the other possibility. *PHACTR4* and *XRCC6*, for example, are highly expressed prenatally compared to other ages, whereas *OPRD1* has the opposite pattern (32, 34, 35). Furthermore, it is unknown if rs678849 mechanisms are limited to certain brain regions or cell types. *OPRD1* expression is limited to a subset of neuronal cell types (36). If the human phenotypes associated with rs678849 genotype are due to *OPRD1* expression differences, future work will need to focus on those specific types of cells.

The most notable limitation of this study is the use of *in vitro* systems. Although our data suggest that the two alleles of rs678849 bind different proteins and have differential effects on transcription, neuroblastoma cells are not a perfect model of normal human tissue. We have attempted to mitigate this issue to the extent possible by confirming the BE(2)C EMSA results using postmortem human brain lysate (Figure 4). However, there is currently limited *in vivo* evidence supporting our observed effect of rs678849 genotype on gene expression. Confirmation of the finding from the BrainSeq consortium or GTEx, or identification of other genes regulated by rs678849 must be a priority for future work. As mentioned, identification of the relevant temporal and spatial parameters will be necessary before this issue can be efficiently addressed. Individuals are also likely to have a wide range of expression levels for any genes of interest due to factors beyond rs678849 genotype and this may make it difficult to directly compare genotypic groups using real-time PCR on bulk lysate. Allelic imbalance assays may therefore be the best way to test this hypothesis and verify that rs678849 is an eQTL in human populations.

Regardless of these considerations, we provide evidence that the alleles of rs678849, an intronic variant associated with buprenorphine effectiveness and addiction-related phenotypes, bind different transcription factors and have differential effects on transcription *in vitro*. These functional differences between the C and T alleles may help explain the psychiatric and neurological phenotype differences predicted by rs678849 genotype.

Supplementary Material

Refer to Web version on PubMed Central for supplementary material.

Funding Source

R.C.C. was supported by NIDA K01 DA036751. R.C.C., W.H.B, and G.A.D. were supported by NIDA R01 DA044015. R.C.C. and W.H.B. were supported by a Pennsylvania CURE grant. B.C.R. was supported, in part, by a 2017 NARSAD Young Investigator Grant (#26634) from the Brain and Behavior Research Foundation as the Patrick A. Coffer Investigator, funding for which was generously provided by Ronald and Kathy Chandonais.

References

1. Kranzler HR, Zhou H, Kember RL, Vickers Smith R, Justice AC, Damrauer S, Tsao PS, Klarin D, Baras A, Reid J, Overton J, Rader DJ, Cheng Z, Tate JP, Becker WC, Concato J, Xu K, Polimanti R, Zhao H, Gelernter J. Genome-wide association study of alcohol consumption and use disorder in 274,424 individuals from multiple populations. Nat Commun 2019; 10 (1), 1499. [PubMed: 30940813]

2. Sanchez-Roige S, Palmer AA, Fontanillas P, Elson SL, Adams MJ, Howard DM, Edenberg HJ, Davies G, Crist RC, Deary IJ, McIntosh AM, Clarke TK. Genome-Wide Association Study Meta-Analysis of the Alcohol Use Disorders Identification Test (AUDIT) in Two Population-Based Cohorts. Am J Psychiatry 2019; 176 (2), 107–118. [PubMed: 30336701]

3. Bierut LJ, Goate AM, Breslau N, Johnson EO, Bertelsen S, Fox L, Agrawal A, Bucholz KK, Grucza R, Hesselbrock V, Kramer J, Kuperman S, Nurnberger J, Porjesz B, Saccone NL, Schuckit M, Tischfield J, Wang JC, Foroud T, Rice JP, Edenberg HJ. ADH1B is associated with alcohol dependence and alcohol consumption in populations of European and African ancestry. Mol Psychiatry 2012; 17 (4), 445–450. [PubMed: 21968928]

4. Crist RC, Doyle GA, Nelson EC, Degenhardt L, Martin NG, Montgomery GW, Saxon AJ, Ling W, Berrettini WH. A polymorphism in the OPRM1 3'-untranslated region is associated with methadone efficacy in treating opioid dependence. Pharmacogenomics J 2016.

5. Hancock DB, Levy JL, Gaddis NC, Glasheen C, Saccone NL, Page GP, Hulse GK, Wildenauer D, Kelty EA, Schwab SG, Degenhardt L, Martin NG, Montgomery GW, Attia J, Holliday EG, McEvoy M, Scott RJ, Bierut LJ, Nelson EC, Kral AH, Johnson EO. Cis-Expression Quantitative Trait Loci Mapping Reveals Replicable Associations with Heroin Addiction in OPRM1. Biol Psychiatry 2015; 78 (7), 474–484. [PubMed: 25744370]

6. Xu J, Lu Z, Xu M, Pan L, Deng Y, Xie X, Liu H, Ding S, Hurd YL, Pasternak GW, Klein RJ, Cartegni L, Zhou W, Pan YX. A heroin addiction severity-associated intronic single nucleotide polymorphism modulates alternative pre-mRNA splicing of the mu opioid receptor gene OPRM1 via hnRNPH interactions. J Neurosci 2014; 34 (33), 11048–11066. [PubMed: 25122903]

7. Crist RC, Clarke TK, Ang A, Ambrose-Lanci LM, Lohoff FW, Saxon AJ, Ling W, Hillhouse MP, Bruce RD, Woody G, Berrettini WH. An intronic variant in OPRD1 predicts treatment outcome for opioid dependence in African-Americans. Neuropsychopharmacology 2013; 38 (10), 2003–2010. [PubMed: 23612435]

8. Crist RC, Phillips KA, Furnari MA, Moran LM, Doyle GA, McNicholas LF, Cornish JW, Kampman KM, Preston KL, Berrettini WH. Replication of the pharmacogenetic effect of rs678849 on buprenorphine efficacy in African-Americans with opioid use disorder. Pharmacogenomics J 2019; 19 (3), 260–268. [PubMed: 30368523]

9. Kranzler HR, Lynch KG, Crist RC, Hartwell E, Le Moigne A, Laffont CM, Andorn AC. A Delta-Opioid Receptor Gene Polymorphism Moderates the Therapeutic Response to Extended-Release Buprenorphine in Opioid Use Disorder. Int J Neuropsychopharmacol 2020.

10. Crist RC, Ambrose-Lanci LM, Vaswani M, Clarke TK, Zeng A, Yuan C, Ferraro TN, Hakonarson H, Kampman KM, Dackis CA, Pettinati HM, O'Brien CP, Oslin DW, Doyle GA, Lohoff FW, Berrettini WH. Case-control association analysis of polymorphisms in the delta-opioid receptor, OPRD1, with cocaine and opioid addicted populations. Drug Alcohol Depend 2013; 127 (1-3), 122–128. [PubMed: 22795689]

11. Sharafshah A, Fazel H, Albonaim A, Omarmeli V, Rezaei S, Mirzajani E, Ajamian F, Keshavarz P. Association of OPRD1 Gene Variants with Opioid Dependence in Addicted Male Individuals Undergoing Methadone Treatment in the North of Iran. J Psychoactive Drugs 2017; 49 (3), 242–251. [PubMed: 28632076]

12. Roussotte FF, Jahanshad N, Hibar DP, Sowell ER, Kohannim O, Barysheva M, Hansell NK, McMahon KL, de Zubicaray GI, Montgomery GW, Martin NG, Wright MJ, Toga AW, Jack CR Jr., Weiner MW, Thompson PM. A commonly carried genetic variant in the delta opioid receptor gene, OPRD1, is associated with smaller regional brain volumes: replication in elderly and young populations. Hum Brain Mapp 2014; 35 (4), 1226–1236. [PubMed: 23427138]

13. Arnoult N, Correia A, Ma J, Merlo A, Garcia-Gomez S, Maric M, Tognetti M, Benner CW, Boulton SJ, Saghatelian A, Karlseder J. Regulation of DNA repair pathway choice in S and G2 phases by the NHEJ inhibitor CYREN. Nature 2017; 549 (7673), 548–552. [PubMed: 28959974]

14. Zhao H, Zhuang Y, Li R, Liu Y, Mei Z, He Z, Zhou F, Zhou Y. Effects of different doses of X-ray irradiation on cell apoptosis, cell cycle, DNA damage repair and glycolysis in HeLa cells. Oncol Lett 2019; 17 (1), 42–54. [PubMed: 30655736]

15. Goldstein RZ, Volkow ND. Dysfunction of the prefrontal cortex in addiction: neuroimaging findings and clinical implications. Nat Rev Neurosci 2011; 12 (11), 652–669. [PubMed: 22011681]

16. Amatu A, Sartore-Bianchi A, Moutinho C, Belotti A, Bencardino K, Chirico G, Cassingena A, Rusconi F, Esposito A, Nichelatti M, Esteller M, Siena S. Promoter CpG island hypermethylation of the DNA repair enzyme MGMT predicts clinical response to dacarbazine in a phase II study for metastatic colorectal cancer. Clin Cancer Res 2013; 19 (8), 2265–2272. [PubMed: 23422094]
17. Mou Z, Hyde TM, Lipska BK, Martinowich K, Wei P, Ong CJ, Hunter LA, Palaguachi GI, Morgun E, Teng R, Lai C, Condarco TA, Demidowich AP, Krause AJ, Marshall LJ, Haack K, Voruganti VS, Cole SA, Butte NF, Comuzzie AG, Nalls MA, Zonderman AB, Singleton AB, Evans MK, Martin B, Maudsley S, Tsao JW, Kleinman JE, Yanovski JA, Han JC. Human Obesity Associated with an Intronic SNP in the Brain-Derived Neurotrophic Factor Locus. Cell Rep 2015; 13 (6), 1073–1080. [PubMed: 26526993]
18. Tolnay M, Vereshchagina LA, Tsokos GC. Heterogeneous nuclear ribonucleoprotein D0B is a sequence-specific DNA-binding protein. Biochem J 1999; 338 (Pt 2), 417–425. [PubMed: 10024518]
19. Tolnay M, Baranyi L, Tsokos GC. Heterogeneous nuclear ribonucleoprotein D0 contains transactivator and DNA-binding domains. Biochem J 2000; 348 Pt 1, 151–158. [PubMed: 10794726]
20. Dempsey LA, Hanakahi LA, Maizels N. A specific isoform of hnRNP D interacts with DNA in the LR1 heterodimer: canonical RNA binding motifs in a sequence-specific duplex DNA binding protein. J Biol Chem 1998; 273 (44), 29224–29229. [PubMed: 9786934]
21. Walker JR, Corpina RA, Goldberg J. Structure of the Ku heterodimer bound to DNA and its implications for double-strand break repair. Nature 2001; 412 (6847), 607–614. [PubMed: 11493912]
22. Mimori T, Hardin JA. Mechanism of interaction between Ku protein and DNA. J Biol Chem 1986; 261 (22), 10375–10379. [PubMed: 3015926]
23. Camara-Clayette V, Thomas D, Rahuel C, Barbey R, Cartron JP, Bertrand O. The repressor which binds the -75 GATA motif of the GPB promoter contains Ku70 as the DNA binding subunit. Nucleic Acids Res 1999; 27 (7), 1656–1663. [PubMed: 10075997]
24. Shi L, Qiu D, Zhao G, Corthesy B, Lees-Miller S, Reeves WH, Kao PN. Dynamic binding of Ku80, Ku70 and NF90 to the IL-2 promoter in vivo in activated T-cells. Nucleic Acids Res 2007; 35 (7), 2302–2310. [PubMed: 17389650]
25. Nolens G, Pignon JC, Koopmansch B, Elmoualij B, Zorzi W, De Pauw E, Winkler R. Ku proteins interact with activator protein-2 transcription factors and contribute to ERBB2 overexpression in breast cancer cell lines. Breast Cancer Res 2009; 11 (6), R83. [PubMed: 19906305]
26. De Zio D, Bordi M, Tino E, Lanzuolo C, Ferraro E, Mora E, Ciccosanti F, Fimia GM, Orlando V, Cecconi F. The DNA repair complex Ku70/86 modulates Apaf1 expression upon DNA damage. Cell Death Differ 2011; 18 (3), 516–527. [PubMed: 20966962]
27. Willis DM, Loewy AP, Charlton-Kachigian N, Shao JS, Ornitz DM, Towler DA. Regulation of osteocalcin gene expression by a novel Ku antigen transcription factor complex. J Biol Chem 2002; 277 (40), 37280–37291. [PubMed: 12145306]
28. Vogel H, Lim DS, Karsenty G, Finegold M, Hasty P. Deletion of Ku86 causes early onset of senescence in mice. Proc Natl Acad Sci U S A 1999; 96 (19), 10770–10775. [PubMed: 10485901]
29. Li GC, Ouyang H, Li X, Nagasawa H, Little JB, Chen DJ, Ling CC, Fuks Z, Cordon-Cardo C. Ku70: a candidate tumor suppressor gene for murine T cell lymphoma. Mol Cell 1998; 2 (1), 1–8. [PubMed: 9702186]
30. Mazumder S, Plesca D, Kinter M, Almasan A. Interaction of a cyclin E fragment with Ku70 regulates Bax-mediated apoptosis. Mol Cell Biol 2007; 27 (9), 3511–3520. [PubMed: 17325036]
31. Cohen HY, Lavu S, Bitterman KJ, Hekking B, Imahiyerobo TA, Miller C, Frye R, Ploegh H, Kessler BM, Sinclair DA. Acetylation of the C terminus of Ku70 by CBP and PCAF controls Bax-mediated apoptosis. Mol Cell 2004; 13 (5), 627–638. [PubMed: 15023334]
32. BrainSeq: Neurogenomics to Drive Novel Target Discovery for Neuropsychiatric Disorders. Neuron 2015; 88 (6), 1078–1083. [PubMed: 26687217]
33. The GTEx Consortium. Human genomics. The Genotype-Tissue Expression (GTEx) pilot analysis: multitissue gene regulation in humans. Science 2015; 348 (6235), 648–660. [PubMed: 25954001]

34. Colantuoni C, Lipska BK, Ye T, Hyde TM, Tao R, Leek JT, Colantuoni EA, Elkahloun AG, Herman MM, Weinberger DR, Kleinman JE. Temporal dynamics and genetic control of transcription in the human prefrontal cortex. Nature 2011; 478 (7370), 519–523. [PubMed: 22031444]

35. Bakalkin G, Yakovleva T, Hurd YL, Nussenzweig A, Li GC, Terenius L. Autoantigen Ku in the brain. Developmentally regulated expression and subcellular localization. Neuroreport 1998; 9 (9), 2147–2151. [PubMed: 9674610]

36. Lake BB, Ai R, Kaeser GE, Salathia NS, Yung YC, Liu R, Wildberg A, Gao D, Fung HL, Chen S, Vijayaraghavan R, Wong J, Chen A, Sheng X, Kaper F, Shen R, Ronaghi M, Fan JB, Wang W, Chun J, Zhang K. Neuronal subtypes and diversity revealed by single-nucleus RNA sequencing of the human brain. Science 2016; 352 (6293), 1586–1590. [PubMed: 27339989]

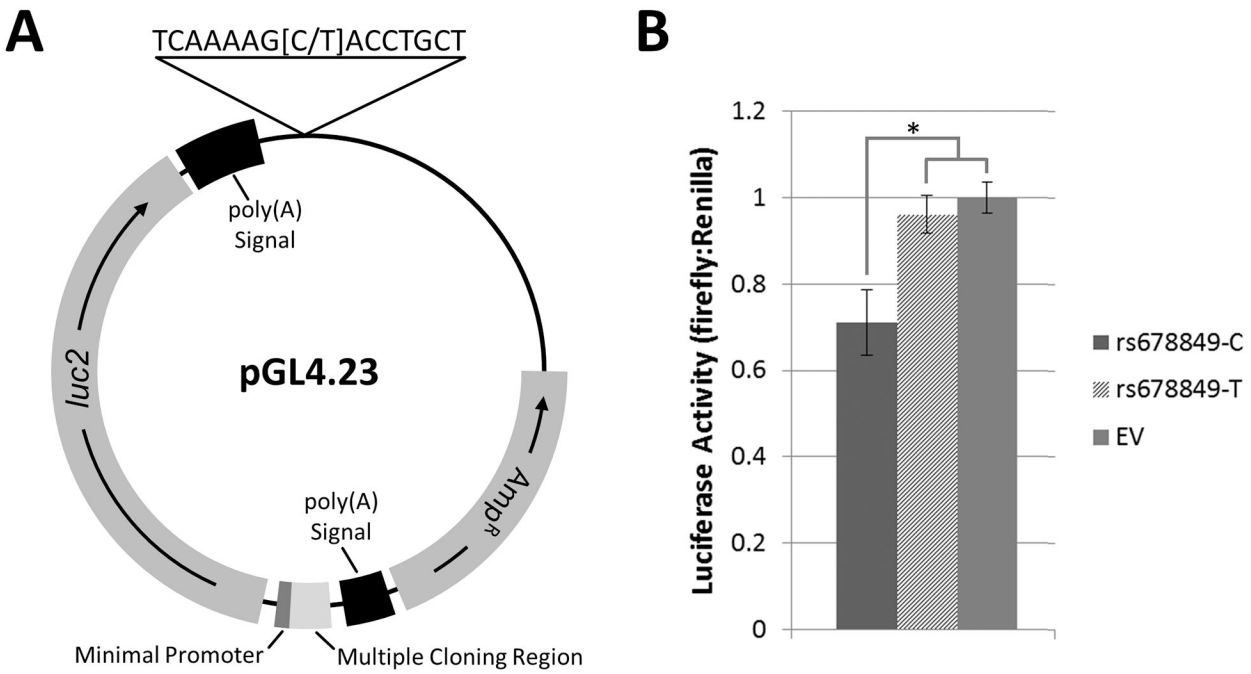

Figure 1:

The C allele of rs678849 acts as a transcriptional silencer *in vitro*. (A) Map of pGL4.23 luciferase construct with location of the inserted rs678849 locus. 15bp sequence containing the C or T allele was cloned into a *Bam*HI site downstream of the *luc2* gene. (B) Luciferase activity in BE(2)C neuroblastoma cells transfected with pGL4.23 rs678849-C, rs678849-T, or empty vector (EV) control. *Renilla* luciferase vector pGL4.74 was co-transfected as a control for transfection efficiency. Ratios of firefly:*Renilla* luciferase activity are presented as mean ± standard deviation (n = 8-9 for all conditions) after normalization to empty vector control. * ANOVA $p < 0.001$

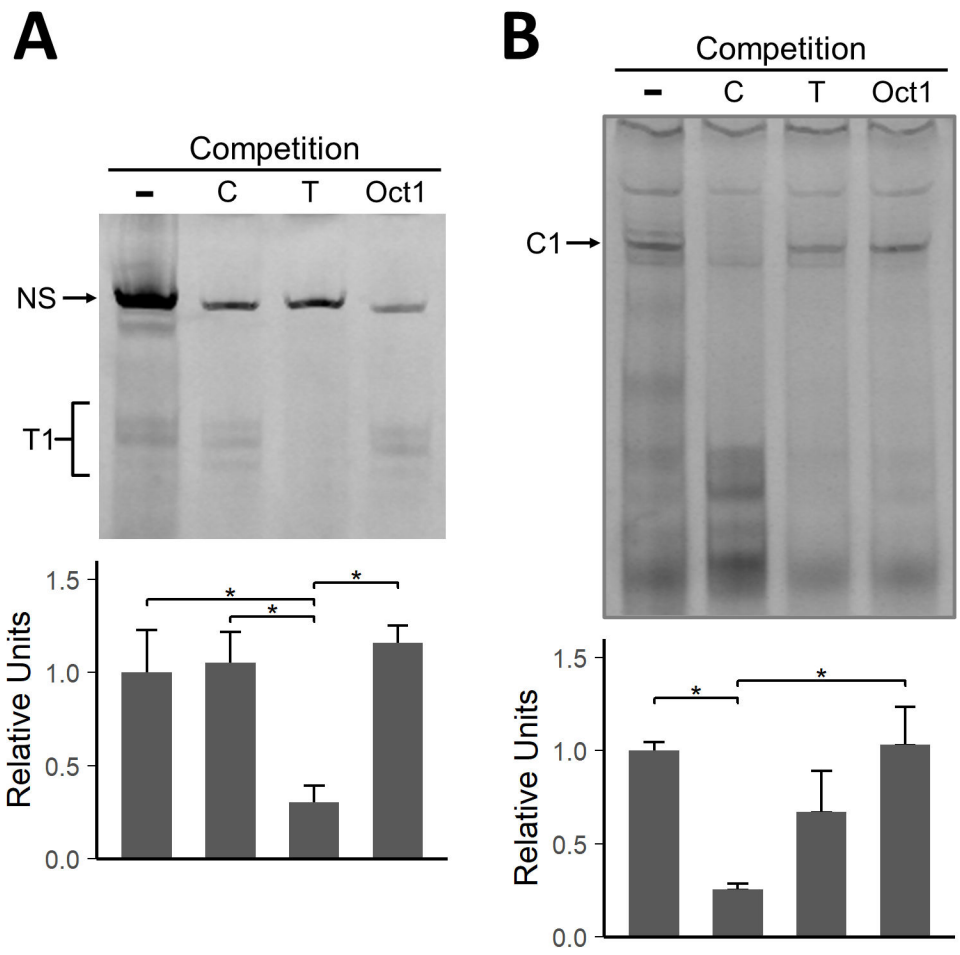

Figure 2:

The T and C alleles of rs678849 bind the sequence-specific protein complexes T1 and C1 in electrophoretic mobility shift assays. (A) Double-stranded, Cy3-labeled DNA probe of the rs678849 T allele was incubated with BE(2)C nuclear lysate in the presence of excess unlabeled C probe (“C”), unlabeled T probe (“T”), or murine Oct1 sequence (“Oct1”). Incubation with no competition was used as a control (“-”). A prominent non-specific band (NS) is observed in all lanes (B) EMSA using a labeled C probe was performed with dephosphorylated BE(2)C nuclear lysate to remove the non-specific band. Competitor sequences were added as described above. Bar plots below the gels indicate the relative intensity (mean ± standard deviation) of the region of interest in each lane, normalized to the lysate control lane (n = 3 for each condition). * ANOVA $p < 0.01$

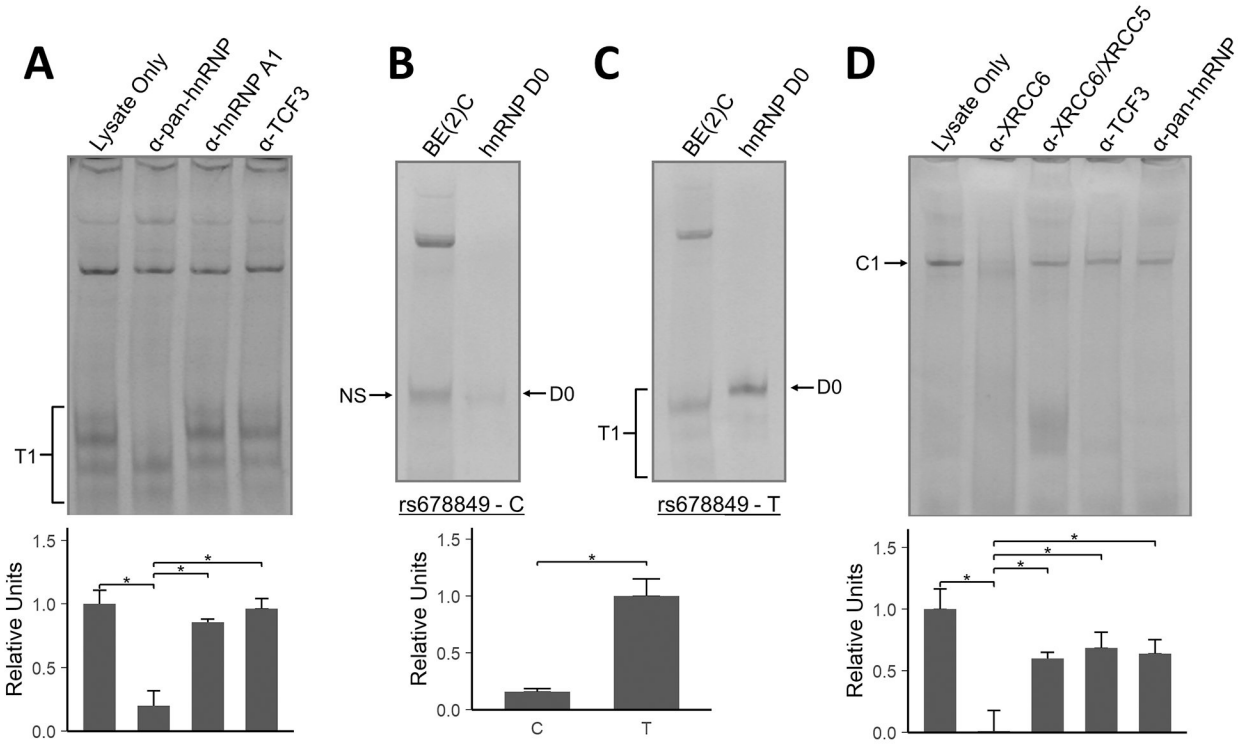

Figure 3:

HnRNP D0 and XRCC6 are components of T1 and C1, respectively. BE(2)C nuclear lysate was incubated with Cy3-labeled dsDNA probes for the T allele (A) and C allele (D) of rs678849 in the presence of excess murine Oct1 sequence. (A) The presence of hnRNP D0 in T1 was examined by the addition of α-pan-hnRNP, α-hnRNP A1, and α-TCF3 antibodies to the EMSA reactions. Incubation of C allele (B) and T allele (C) probes with BE(2)C nuclear lysate or Myc-DDK-tagged recombinant hnRNP D0 further demonstrated preference of the protein for the T allele. Note that the recombinant hnRNP D0 does not match the migration of the endogenous hnRNP D0 due to the presence of the Myc-DDK tag. NS: Non-specific protein complex running at approximately the size of the Myc-DDK-tagged hnRNP D0 in the presence of the C probe. (D) The presence of XRCC6 in the C1 complex was examined by the addition of α-XRCC6, α-XRCC6/XRCC5, α-TCF3, and α-pan-hnRNP antibodies. Bar plots below the gels indicate the relative intensity (mean ± standard deviation) of the region of interest in each lane, normalized to the lysate control lane (n = 3 for each condition). * ANOVA $p < 0.01$

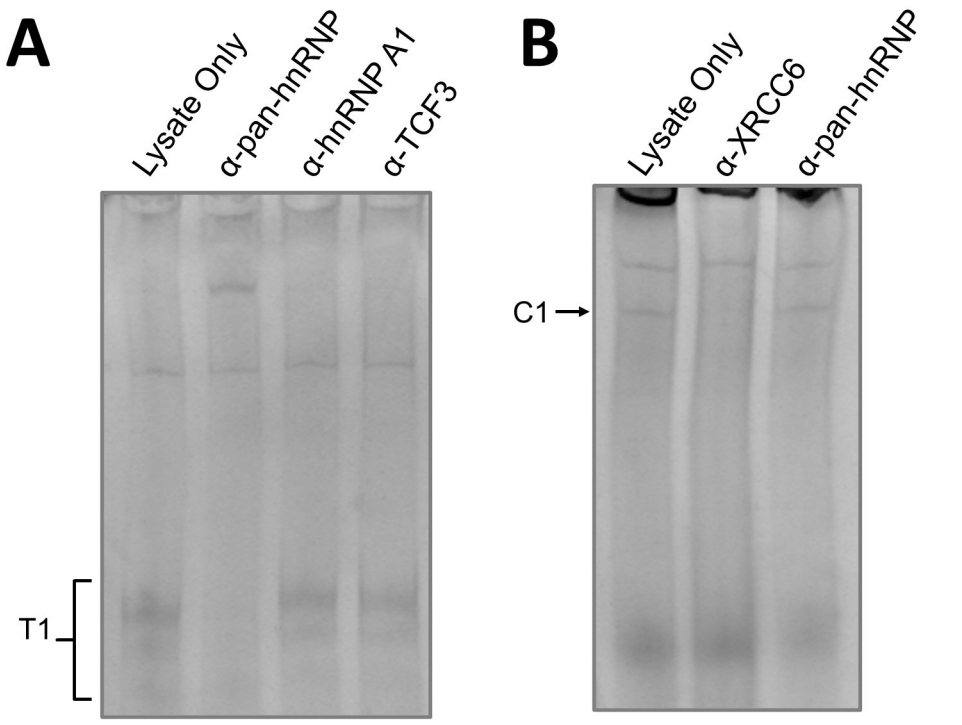

Figure 4:

T1 and C1 are present in postmortem human brain and contain hnRNP D0 and XRCC6, respectively. Nuclear lysate from postmortem human medial prefrontal cortex was incubated with Cy3-labeled dsDNA probes for the T allele (A) and C allele (B) of rs678849 in the presence of excess murine Oct1 sequence. (A) The presence of hnRNP D0 was examined by the addition of α-pan-hnRNP, α-hnRNP A1, and α-TCF3 antibodies to the EMSA reactions. (B) The presence of XRCC6 in the C1 complex was examined by the addition of α-XRCC6 and α-pan-hnRNP antibodies. Dephosphorylated nuclear lysate was used to remove the non-specific band and maintain consistency with the BE(2)C analyses. Presence or absence of the relevant protein complexes was assessed qualitatively.

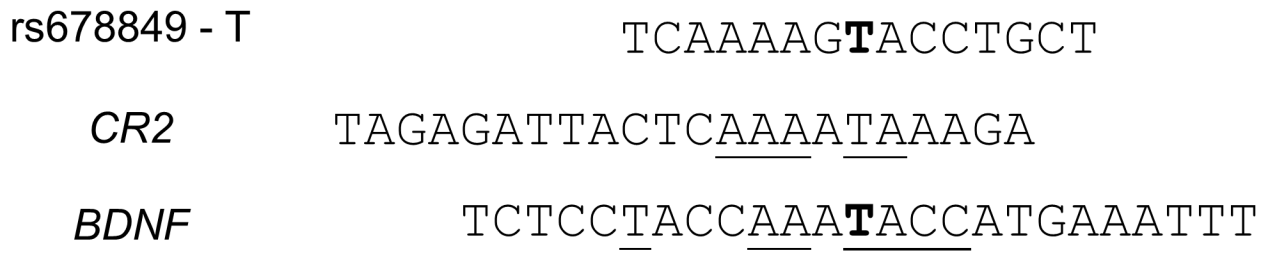

Figure 5:

Overlap between the T allele probe for rs678849 and known binding sites for isoform 3 of hnRNP D0 in *CR2* and *BDNF*. Bases matching the rs678849 locus are underlined. The bolded bases indicate rs678849 in *OPRD1* and rs12291063 in *BDNF*.